Molecular Vision 2015; 21:1345-1356 <http://www.molvis.org/molvis/v21/1345>
Received 13 August 2015 | Accepted 28 December 2015 | Published 30 December 2015

Optimization of immunostaining on flat-mounted human corneas

Fabien Forest,[1,2] Gilles Thuret,[1,3] Philippe Gain,[1] Jean-Marc Dumollard,[1,2] Michel Peoc'h,[1,2] Chantal Perrache,[1] Zhiguo He[1]

[1]"Corneal Graft Biology, Engineering and Imaging" Laboratory, EA2521, SFR 143, Faculty of Medicine, Jean Monnet University, Saint-Etienne, France; [2]Department of Pathology, University Hospital of Saint-Etienne, France; [3]Institut Universitaire de France, Paris, France

Purpose: In the literature, immunohistochemistry on cross sections is the main technique used to study protein expression in corneal endothelial cells (ECs), even though this method allows visualization of few ECs, without clear subcellular localization, and is subject to the staining artifacts frequently encountered at tissue borders. We previously proposed several protocols, using fixation in 0.5% paraformaldehyde (PFA) or in methanol, allowing immunostaining on flatmounted corneas for proteins of different cell compartments. In the present study, we further refined the technique by systematically assessing the effect of fixative temperature. Last, we used optimized protocols to further demonstrate the considerable advantages of immunostaining on flatmounted intact corneas: detection of rare cells in large fields of thousands of ECs and epithelial cells, and accurate subcellular localization of given proteins.

Methods: The staining of four ubiquitous proteins, ZO-1, hnRNP L, actin, and histone H3, with clearly different subcellular localizations, was analyzed in ECs of organ-cultured corneas. Whole intact human corneas were fixed for 30 min in 0.5% paraformaldehyde or pure methanol at four temperatures (4 °C for PFA, −20 °C for methanol, and 23, 37, and 50 °C for both). Experiments were performed in duplicate and repeated on three corneas. Standardized pictures were analyzed independently by two experts. Second, optimized immunostaining protocols were applied to fresh corneas for three applications: identification of rare cells that express KI67 in the endothelium of specimens with Fuch's endothelial corneal dystrophy (FECD), the precise localization of neural cell adhesion molecules (NCAMs) in normal ECs and of the cytokeratin pair K3/12 and CD44 in normal epithelial cells, and the identification of cells that express S100b in the normal epithelium.

Results: Temperature strongly influenced immunostaining quality. There was no ubiquitous protocol, but nevertheless, room temperature may be recommended as first-line temperature during fixation, instead of the conventional −20 °C for methanol and 4 °C for PFA. Further optimization may be required for certain target proteins. Optimized protocols allowed description of two previously unknown findings: the presence of a few proliferating ECs in FECD specimens, suggesting ineffective compensatory mechanisms against premature EC death, and the localization of NCAMs exclusively in the lateral membranes of ECs, showing hexagonal organization at the apical pole and an irregular shape with increasing complexity toward the basal pole. Optimized protocols were also effective for the epithelium, allowing clear localization of cytokeratin 3/12 and CD44 in superficial and basal epithelial cells, respectively. Finally, S100b allowed identification of clusters of epithelial Langerhans cells near the limbus and more centrally.

Conclusions: Fixative temperature is a crucial parameter in optimizing immunostaining on flatmounted intact corneas. Whole-tissue overview and precise subcellular staining are significant advantages over conventional immunohistochemistry (IHC) on cross sections. This technique, initially developed for the corneal endothelium, proved equally suitable for the corneal epithelium and could be used for other superficial mono- and multilayered epithelia.

The corneal endothelium, a monolayer of tightly packed hexagonal flat cells at the posterior surface of the cornea, is crucial for maintaining corneal transparency. Possibilities for analyzing the protein expressed in corneal endothelial cells (ECs) are limited by their small number (300,000 to 500,000 per cornea). Protein extraction for immunoblots is not the current technique and has been reported only after several donors' ECs are pooled [1-4]. Immunostaining techniques are therefore those most widely used to study protein expression in situ. In the literature, the robust technique of immunohistochemistry (IHC) on cross sections is the main technique used for the corneal endothelium because IHC is simple, despite allowing visualization of only a few ECs, without clear subcellular localization, and being subject to the staining artifacts frequently encountered at tissue borders. To avoid these drawbacks, we previously developed specific immunostaining protocols performed directly on the intact endothelium of the whole cornea to allow en face viewing [5] without a tissue cross section. This technique has two main advantages: striking visualization of the whole intact endothelium, allowing detection of regional or local differences

Correspondence to: Gilles Thuret, "Corneal Graft Biology, Engineering and Imaging" Laboratory, EA 2521, IFR 143, Faculty of Medicine, 10 rue de la Marandière, BP 80019, 42055 Saint-Etienne, France, Phone:+33 (0) 477421425 ; FAX: +33 (0)4 77 12 05 49; email: gilles.thuret@univ-st-etienne.fr

Table 1. Primary antibodies.

Target proteins	Animal source	Clone	Manufacturer
ZO-1	mouse	ZO1–1A12	Zymed, Carlsbad, CA
actin	rabbit	polyclonal	Sigma, Saint Louis, MO
hnRNP L	mouse	4D11	Abcam, Cambridge, UK
histone H3	rabbit	polyclonal	Abcam
Ki67	mouse	MIB-1	Dako, Glostrup, Denmark
NCAM	mouse	301,021	R&D systems, Minneapolis, MN
Cytokeratin3+12	mouse	2Q1040	Abcam
CD44	mouse	F10–44–2	Abcam
S-100*	rabbit	polyclonal	Dako

*according to DAKO: reacts with S100B strongly, S100A1 weakly, and S100A6 very weakly. No reaction was observed with the other S100 proteins tested, S100A2, S100A3 and S100A4

in staining patterns (up to the easy detection of isolated rare cells with a specific expression profile, such as the detection of rare stem-like cells within the endothelium [6]) and precise subcellular localization.

The technique is an IHC/immunocytochemistry hybrid, because it concerns a cell monolayer on top of intact tissue. We demonstrated that cells were easily overfixed in the flatmounted cornea, resulting in poor-quality immunostaining when the cornea is treated with conventional 4% paraformaldehyde (PFA), which suits most cases of IHC on solid tissues and of immunocytochemistry (ICC) on cultured cells. Instead, we showed that 0.5% PFA and pure methanol, each for 30 min at room temperature (RT, 23 °C), were the first-choice fixatives to perform immunostaining on intact ECs of flatmounted whole corneas. Nevertheless, during this study, we observed that the temperature during fixation may often strongly influence staining quality [5]. For diverse immunostaining techniques, such as IHC and ICC, the recommended temperature during fixation is −20 °C for methanol and 4 °C for PFA, although the influence of temperature on staining quality has not been clearly reported [7].

To study the influence of temperature during fixation on staining quality and further improve immunostaining of ECs on flatmounted corneas, we systematically assessed a wide range of temperatures during methanol and PFA fixation for the labeling of four proteins located in different cell compartments. Second, to illustrate the advantages of this optimized technique, we identified rare proliferating cells in the endothelium of specimens of Fuchs' endothelial corneal dystrophy (FECD), which is the most common primary endothelial dystrophy and a leading indication for keratoplasty, and characterized the three-dimensional (3D) shape of the lateral membranes of ECs using neural cell adhesion molecule (NCAM) labeling. Finally, we investigated the application of this technique to the corneal epithelium.

METHODS

Human corneas: Ten organ cultured (OC) human corneas were used for fixative temperature testing. Storage time was (mean±standard deviation, SD) 22±10 days (7 to 35, median 21). Endothelial cell density (ECD) was 1,976±618 cells/mm^2 (1,229 to 2,898, median 2004). The corneas were obtained from seven donors aged 75±8 years (54 to 81, median 77). Two pairs of fresh corneas were used for NCAM, cytokeratin 3/12, and S100 staining. Donor ages were 73 and 68 years, and time from death to procurement was 9 and 23 h, respectively. Two corneal buttons with FECD were used. They were obtained from the operating theater, with 45 min from excision to fixation. Patient ages were 61 and 68 years. All OC corneas were obtained from the Eye Bank of Saint-Etienne and initially stored in 100 mL organ culture medium (CorneaMax, Eurobio, Les Ulis, France) at 31 °C without medium renewal. All fresh corneas were procured from bodies donated to science (Laboratory of Anatomy, Faculty of Medicine) as permitted by the French bioethics law. Donors volunteer their body and give written consent to the Laboratory of Anatomy; no further specific approval by the ethics committee is required. The study was conducted in accordance with the ARVO statement for the use of human subjects in Ophthalmic and Vision research. Handling of donor tissues adhered to the tenets of the Declaration of Helsinki of 1975 and its 1983 revision in protecting donor confidentiality.

Antibodies: Specific primary antibodies for this study are presented in Table 1. Whenever possible, they were chosen among antibodies validated by their manufacturers for ICC, which seemed closest to our technique. Non-specific rabbit

and/or mouse immunoglobulin G (IgG; Zymed, Carlsbad, CA) were used as primary antibodies for negative controls (i.e., secondary antibody control [8]). Secondary antibodies were Alexa Fluor 488 goat anti-mouse IgG or/and Alexa Fluor 555 goat anti-rabbit IgG (Invitrogen, Eugene, OR). Four proteins known to be consistently expressed in ECs with a characteristic pattern or ubiquitous proteins were chosen: ZO-1 is a peripheral membrane protein associated with tight junctions [9]; actin is one of the most conserved cytoplasmic proteins in eukaryotes, and its particularity in ECs is hexagonal shaped distribution [10]; heterogeneous ribonucleoprotein L (hnRNP L) is present in the nucleoplasm as part of the hnRNP complexes that play a major role in the formation, packaging, processing, and function of mRNA; and histone H3 is one of the basic nuclear proteins responsible for the nucleosome structure of chromosomal fibers in eukaryotes.

Immunostaining on flatmounted whole corneas: The general processing of corneas followed previously described protocols [5] and is summarized in Figure 1. Briefly, corneas were rinsed in PBS (1X; 140 mM NaCl, 3 mM KCl, 10 mM $NaPO_4$, pH 7.4 at 25 °C), cut into four to eight pie-shaped wedges to increase the number of experiments while saving rare tissue, and fixed immediately after removal from the OC medium. Double staining was chosen, again to save the human corneas. Fixation was performed for 30 min either in 0.5% PFA in PBS pH 7.45 at 4 °C, RT, 37 °C or 50 °C, or in methanol at −20 °C, RT, 37 °C or 50 °C. For the PFA-fixed corneas, the cell membranes were then permeabilized using 1% Triton x-100 in PBS for 5 min at RT, except histone H3 labeling for which we previously showed that antigen retrieval with 1% sodium dodecyl sulfate (SDS) in water for 5 min at RT was necessary [5]. The non-specific binding sites were then blocked by incubation for 30 min at 37 °C with blocking buffer based on PBS supplemented with 2% heat-inactivated goat serum and 2% bovine serum albumin (BSA). All primary antibodies were diluted 1:200 in the blocking buffer. The corneal pieces were fully immersed in this solution and incubated at 37 °C for 1 h. Incubation with secondary antibodies diluted at 1:500 in blocking buffer was done for 45 min at 37 °C. Nuclei were finally counterstained with Hoechst 33,342 (Sigma) 10 µg/ml in PBS at RT for 2 min. Three rinses in PBS were performed between each step, except between blocking of non-specific protein binding sites and incubation with the primary antibody. The corneal piece was last placed on a glass slide, covered with PBS, and gently

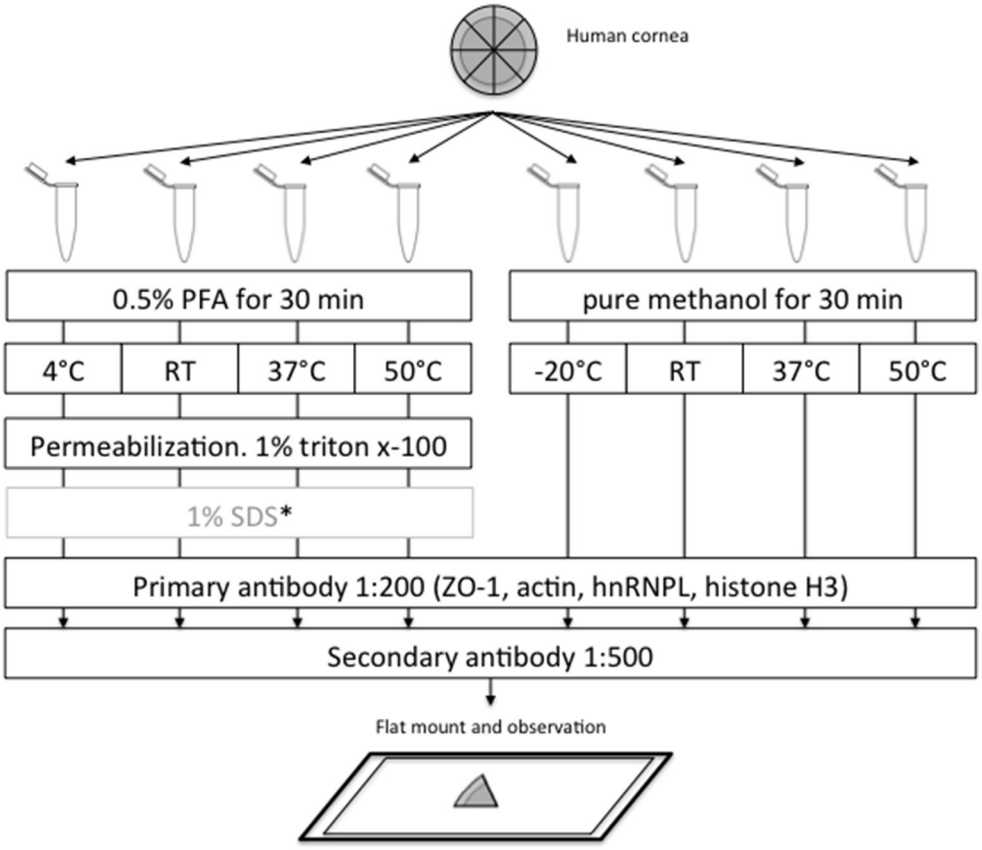

Figure 1. Schematics of the experiments designed for optimizing immunostaining on flatmounted whole corneas. Four fixation temperatures were assessed for each of the two fixatives. Only the main steps are presented. For details, refer to the Methods section. *Antigen retrieval using sodium dodecyl sulfate (SDS) was used only for revealing histone H3. room temperature=RT.

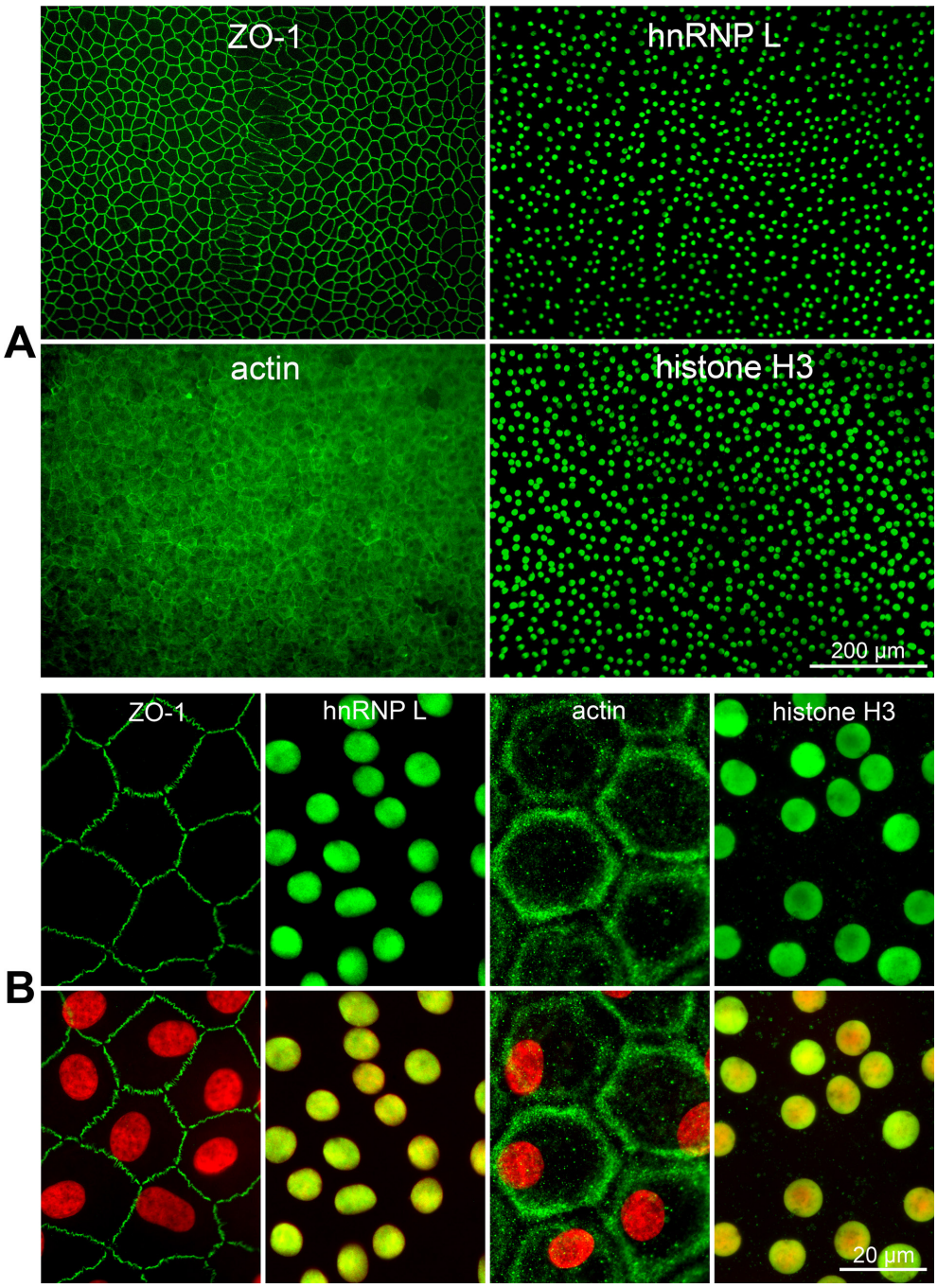

Figure 2. Best results obtained after optimization of fixative temperature for detection in corneal ECs of flatmounted human corneas of ZO-1 (methanol at −20 °C), hnRNP L (paraformaldehyde at room temperature [RT]), actin (methanol at 37 °C), and histone H3 (paraformaldehyde at RT + antigen retrieval with sodium dodecyl sulfate). **A**: Low magnification (10X objective) shows homogeneous staining in all endothelial cells (ECs). **B**: High magnification (100X objective) shows the typical staining patterns for each target protein. Upper line: immunostaining alone pseudocolored in green; lower line: merge with nuclei, labeled with Hoechst 33,342, pseudocolored in red.

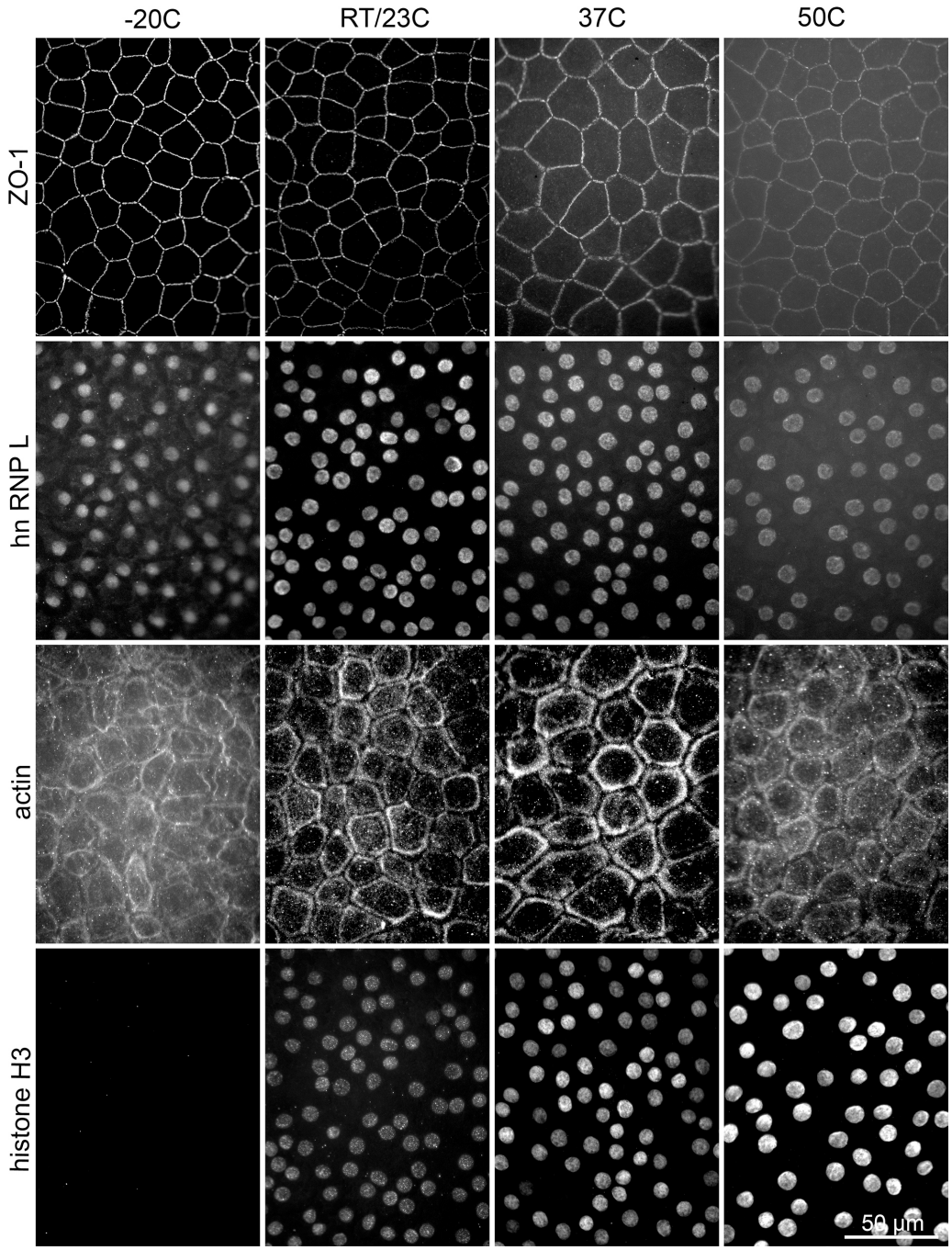

Figure 3. Influence of temperature during methanol fixation. All corneal pieces were fixed for 30 min. No pseudocolor for immunostaining; no counterstaining for nuclei. 40X objective.

flattened using a large glass coverslip held by adhesive tape. Experiments were done at RT unless otherwise stated.

Evaluation of immunostaining quality: Images were captured with an inverted fluorescence microscope IX81 (Olympus, Tokyo, Japan) equipped with the Cell^P imaging software (Soft Imaging System GmbH, Munster, Germany). This non-confocal microscope was chosen to obtain, at low magnification, large-field images able to tolerate the residual 3D aspect of cell layers after flatmounting. Each temperature assay was done in duplicate on the same cornea and repeated at least three times on three different corneas.

During image acquisition, the fluorescence intensity and camera exposure parameters were constant for the same antibody. The immunostaining was evaluated independently by two pathologists experienced in immunofluorescence assessment (FF and JMD), on digital pictures blind to the preparation used. The intensity of staining was rated as null, weak, medium, good, or excellent. In the case of disagreement, a third pathologist (MP) reviewed the pictures.

Applications: The performance of optimized immunostaining protocols was illustrated through three applications: detection of isolated cells among the whole endothelium or epithelium, high-resolution subcellular localization of a membrane bound protein in ECs, and characterization of each epithelial layer. For the first application, the endothelium of the corneal buttons from patients with advanced FECD were labeled for Ki67, a ubiquitous proliferating marker. We hypothesized that the increased rate of apoptosis among ECs [11] could be partly offset by abnormal proliferation. For the epithelium, labeling of the S100B protein, a marker for Langerhans cells and melanocytes, aimed to characterize their distribution within the corneal surface. For the second application, we studied the distribution of the NCAMs, a marker of the neuroectodermic origin of the endothelium [12]. For the third application, the corneas were simply labeled for cytokeratin 3/12 [13] (the superficial layer) and CD44 [14] (the basal layer) and observed at several depths. For each labeling, the best protocol was determination using OC corneas (data not shown). Thereafter, fresh corneas with short post-mortem (or post-operative) times were used as stated above (see the human cornea) to avoid potential artifacts caused by storage in the culture medium. The staining assays were repeated at least twice on three corneas.

RESULTS

Influence of fixative temperature: By optimizing the fixative temperature for each of the four proteins, we obtained striking typical staining patterns in the ECs, in terms of the signal-to-noise ratio and precise subcellular localization. This technique gave an overall view of the endothelium (Figure 2A) and precise subcellular staining (Figure 2B). Under high magnification (96X immersion objective), we observed the typical distribution of ZO-1, with a zigzag pattern between two neighboring cells and absent at the Y junction between three neighboring cells (Figure 2B).

Staining quality after fixation with methanol was particularly dependent on temperature (Figure 3 and Table 2). The conventional temperature of −20 °C was optimal only for ZO-1 and failed with histone H3. Room temperature was optimal for hnRNPL, and 37 °C was optimal for actin. Interestingly, histone H3 was perfectly revealed after fixation at 50 °C, a temperature never before reported for methanol.

Staining quality after fixation with PFA was less blatantly dependent on temperature, but the conventional temperature of 4 °C was optimal only for ZO-1; RT and 37 °C were optimal for hnRNPL. None of the four temperatures allowed revelation of actin and histone H3. Antigen retrieval with 1% SDS allowed clear labeling of histone H3 following PFA fixation at RT and 37 °C but triggered EC detachment after fixation at 4 °C and completely lost its antigen retrieval capability after fixation at 50 °C (Figure 4 and Table 2). No labeling of actin was obtained with any fixative temperature, even after antigen retrieval with SDS.

Table 2. Evaluation of immunostaining at different temperatures with methanol and paraformaldehyde fixation.

Target proteins	Methanol				0.5% paraformaldehyde			
	−20 °C	RT	37 °C	50 °C	4 °C	RT	37 °C	50 °C
ZO-1	++++	+++	++	+	++++	+++	++	+
hnRNP L	++	+++	++	+	++	++++	++++	+
actin	+	+++	++++	++	-	-	-	-
histone H3	-	++	+++	++++	D	++++	++++	-

-: null; +: weak, ++: medium; +++: good; ++++: excellent; D: detachment of endothelial cells by sodium dodecyl sulfate; RT: room temperature.

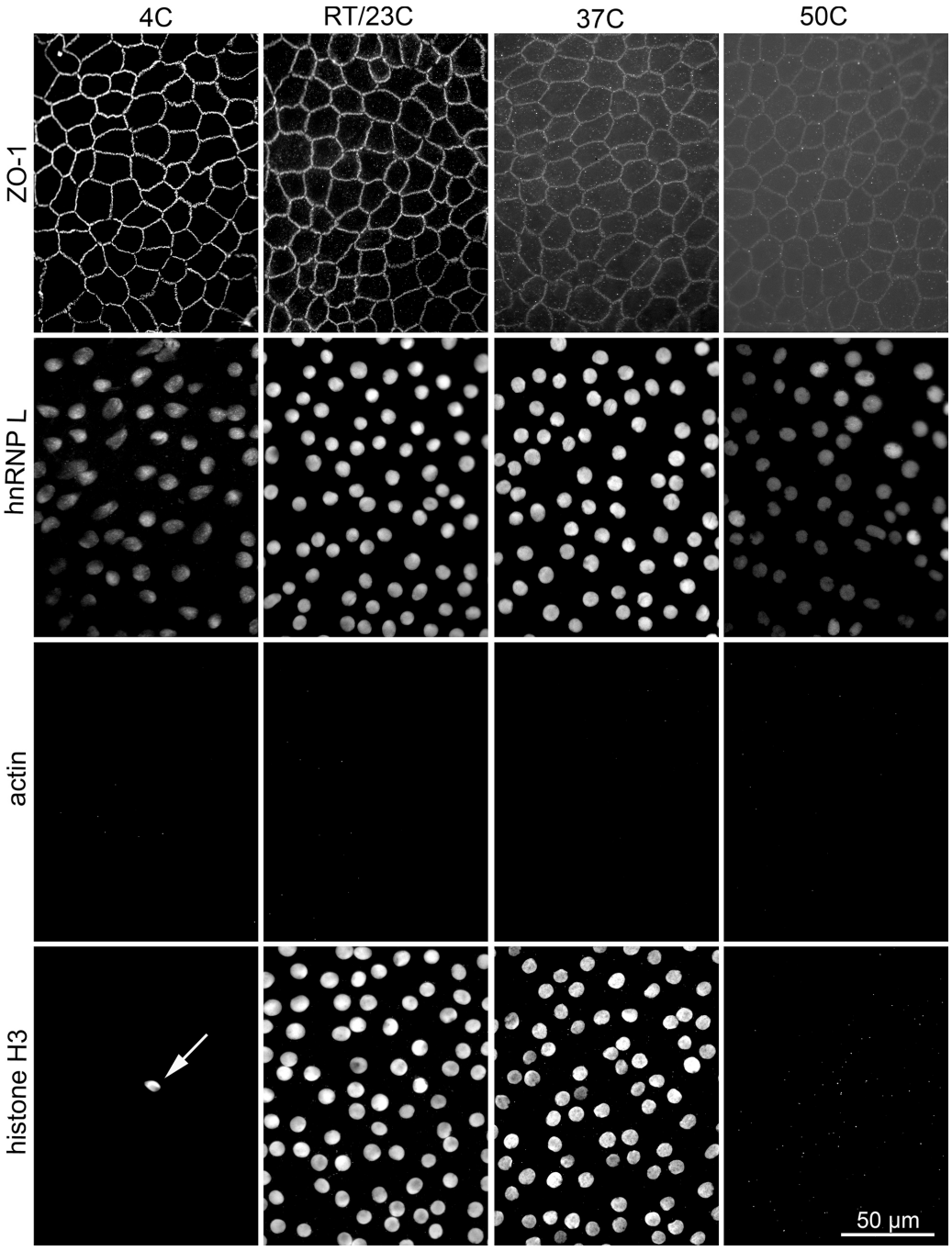

Figure 4. Influence of the temperature during 0.5% paraformaldehyde fixation. All corneal pieces were fixed for 30 min. Antigen retrieval with sodium dodecyl sulfate was efficient only for histone H3, but detached almost all endothelial cells from the Descemet membrane after fixation at 4 °C; the arrow indicates the single cell that remained attached. No pseudocolor for immunostaining; no counterstaining for nuclei. 40X objective.

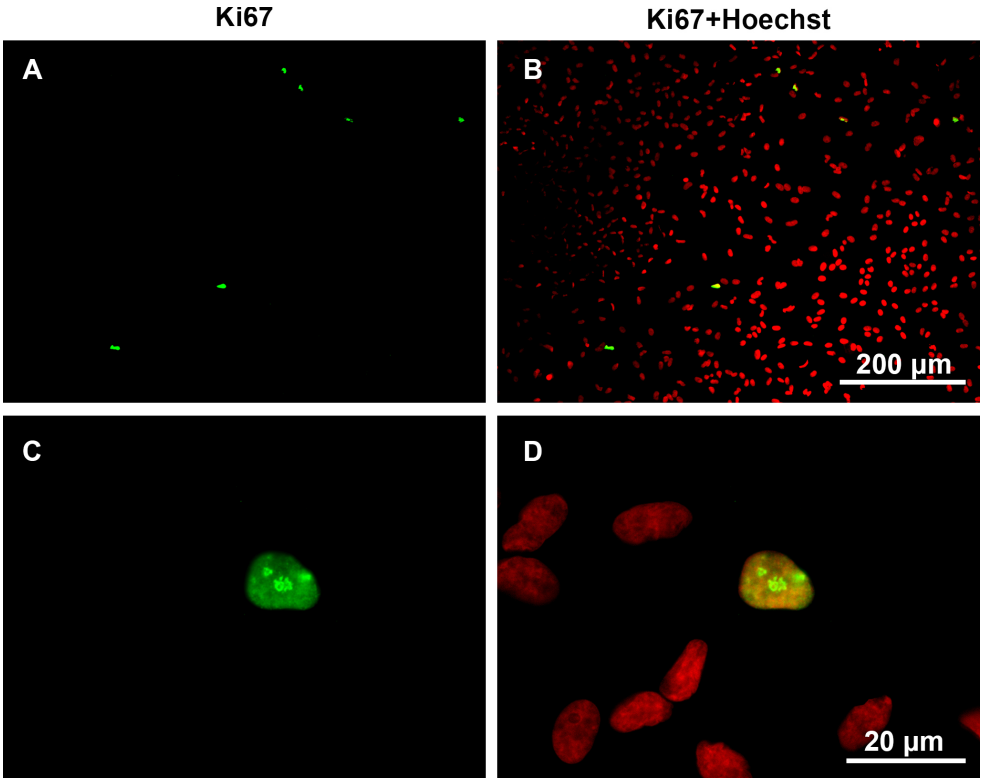

Figure 5. Detection of the expression of the proliferation marker Ki67 in endothelial cells of corneal buttons with Fuchs endothelial corneal dystrophy. **A, B**: Low magnification (10X objective) shows a few Ki67 positive cells scattered at random. Note that the nuclei morphology and distribution of residual endothelial cells are typical of Fuchs' corneal endothelial dystrophy (FECD), with elongated nuclei, areas deprived of cells, and the rosette formation around Descemet excrescences forming the guttae. **C, D**: At high magnification (100X objective), the localization of Ki67 within the nucleolus indicates the S phase of the cell cycle. Ki67 labeling is pseudocolored in green; the nuclei, labeled by Hoechst 33342, are pseudocolored in red.

Applications: The best labeling of Ki67 within the endothelium of the FECD specimens was obtained with PFA fixation at RT. A few proliferating Ki67 positive cells were detected scattered in the endothelium, with a typical staining pattern of the nucleus indicating entry in the S phase of the cell cycle [15]. They were within the endothelial layer, not foreign cells attached to the endothelium, and therefore likely to be ECs (Figure 5).

For NCAM labeling of normal ECs, the optimal protocol was fixation in methanol at 37 °C. Low (10X objective) and intermediate (40X objective) magnification showed that all ECs homogeneously expressed NCAMs; at high magnification (100X objective, NA 1.4), the NCAMs were localized in the lateral membrane and highlighted a strong increase in the irregularity of membrane organization from the apical to the basal cell pole (Figure 6). Furthermore, lateral cell–cell junctions were not always continuous, delimiting some small spaces between neighboring cells. Epithelial cells from the same corneas did not express NCAMs (data not shown).

For cytokeratin 3/12 and S100, PFA fixation at RT was optimal, whereas for CD44, the best staining was obtained with methanol fixation at RT (Figure 7). The typical morphology of the two epithelial populations was perfectly highlighted: The cytoplasm of the large irregular superficial cells was filled by cytokeratin 3/12, and the membranes of the small regular basal cells contained CD44. Some non-epithelial cells with typical dendritic/Langerhans-morphology were highlighted by S100B. They were mainly localized in and around the limbus and scattered in the peripheral and central epithelium.

DISCUSSION

In this study, we demonstrated the strong influence of temperature during fixation for immunostaining of ECs on flatmounted human corneas. In the case of a superficial cell layer such as ECs, directly accessible to fixatives, the fixation process is supposed to be extremely rapid whatever the fixative. Nevertheless, we found substantial temperature-related differences between methanol and formaldehyde.

Methanol is commonly used during ICC on in vitro–cultured cells and sometimes during IHC on frozen tissue cross sections. Classified as a precipitating or agglutinating fixative, methanol reduces protein solubility by creating non-covalent bonds between them. Furthermore, methanol's hydrophilic group (-OH) disrupts the hydrogen bonds between amide groups in the secondary protein structure, and the hydrophobic group (-CH3) disrupts the intramolecular hydrophobic interactions of the protein core and thus denatures the proteins by changing their secondary and

tertiary structures [16]. The temperature −20 °C, commonly used for tissue fixation during immunostaining, was efficient only for detecting ZO-1, whereas RT (23 °C), 37 °C, and 50 °C were adapted to hnRNPL, actin, and histone H3, respectively. This suggests that antigen retrieval by methanol depends on temperature, which may induce different degrees of protein denaturation and thus influence epitope exposure of the various proteins by modifying their secondary and/or tertiary structures. Methanol may not only ensure fixation and antigen retrieval of proteins but also lower the denaturation temperature of DNA [17]. The good results obtained with methanol at 50 °C for labeling of histone H3 were thus probably due to the denaturation of histone H3 and DNA.

For PFA, we demonstrated that, with the 0.5% concentration, RT and 37 °C are more efficient than 4 °C, albeit the recommended temperature. The worst results were obtained at 50 °C, which may accelerate protein cross-linking, resulting in overfixation. However, actin and histone H3 were not revealed by PFA fixation alone. Contrary to methanol that denaturates proteins, formaldehyde cross-links amino groups of proteins with other nearby nitrogen atoms in proteins or DNA through a -CH2- covalent linkage and thus preserves the secondary and tertiary structures of proteins [18]. Recognized epitopes of actin and histone H3 may be hidden in their natural structure and require antigen retrieval [19]. For histone H3, this was achieved using SDS, which disrupts non-covalent bonds in the proteins, between the proteins, and between the proteins and the other molecules such as DNA [20,21]. Nevertheless, SDS was efficient only on corneas fixed at RT and 37 °C. At 4 °C, SDS triggered detachment of ECs, whereas at 50 °C overfixation prevented SDS from unveiling epitopes. Surprisingly, for actin, antigen retrieval by SDS remained inefficient. The lower performance of PFA

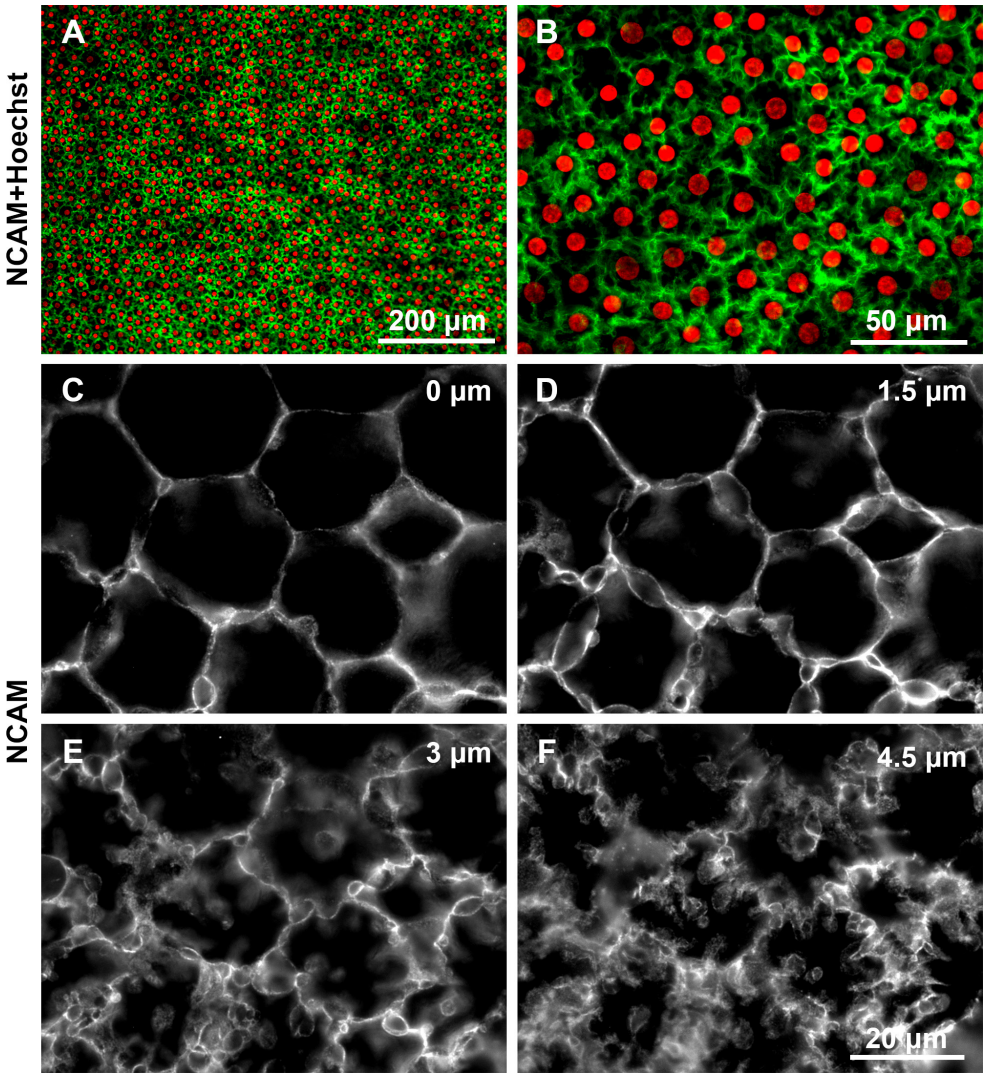

Figure 6. Expression of neural cell adhesion molecule (NCAM) in endothelial cells (ECs) of a fresh normal cornea. **A**, **B**: Low magnification (10X objective) shows homogeneous expression of NCAMs in all ECs while medium magnification (40X objective) reveals irregular organization of the lateral membrane where the NCAMs are located. The NCAMs are pseudocolored in green. The nuclei, labeled by Hoechst 33342, are pseudocolored in red. **C**–**F**: High magnification (100X objective) shows continuous expression of the NCAMs at increasing depths from the apical pole of the ECs, unveiling the increasingly irregular organization of the lateral membranes from the apical to basal pole.

in revealing actin compared to that of methanol fixation was reported previously without a clear explanation [22].

Normal ECs are arrested during the G1 phase of the cell cycle in human adults [23]. With immunostaining on flat-mounted whole corneas, we did not find any proliferating cells expressing Ki67 on the central and peripheral endothelium [5] except at the extreme periphery of the endothelium on fresh corneas with a death to procurement time of less than 6 h [6]. Fuchs' dystrophy is a degenerative disease of the corneal endothelium, and the pathogenesis is still largely unknown. A continuous decrease in cell density due to EC apoptosis is suspected [11]. For the first time, we labeled some proliferating cells suggesting that abnormal cell proliferation may be a factor in slowing down EC loss.

NCAM expression in human ECs was first described by Foets et al. in 1992 [12]. Probably because of the non-optimal immunostaining protocol, NCAM expression seemed heterogeneous and the subcellular localization imprecise. Here, we showed strong and homogenous expression of NCAMs, exclusively on the lateral membranes of ECs of fresh corneas, and the absence of expression in the corneal epithelium, contrary to ZO-1 and Na^+/K^+ ATPase, currently used as standard EC markers [24,25], but also expressed in the corneal epithelium. We therefore suggest using NCAMs as a new marker for distinguishing endothelial and epithelial cells, in particular during in vitro bioengineering of the corneal endothelium. Usually, ECs are seen as hexagonal flat cells, but this feature characterizes only the apical pole. The ultrastructure of their interdigitated lateral borders was already shown by transmission electron microscopy on corneal cross sections [26-28], but never before has the precise en face view of the lateral membrane been clearly described with light microscopy. Because this technique

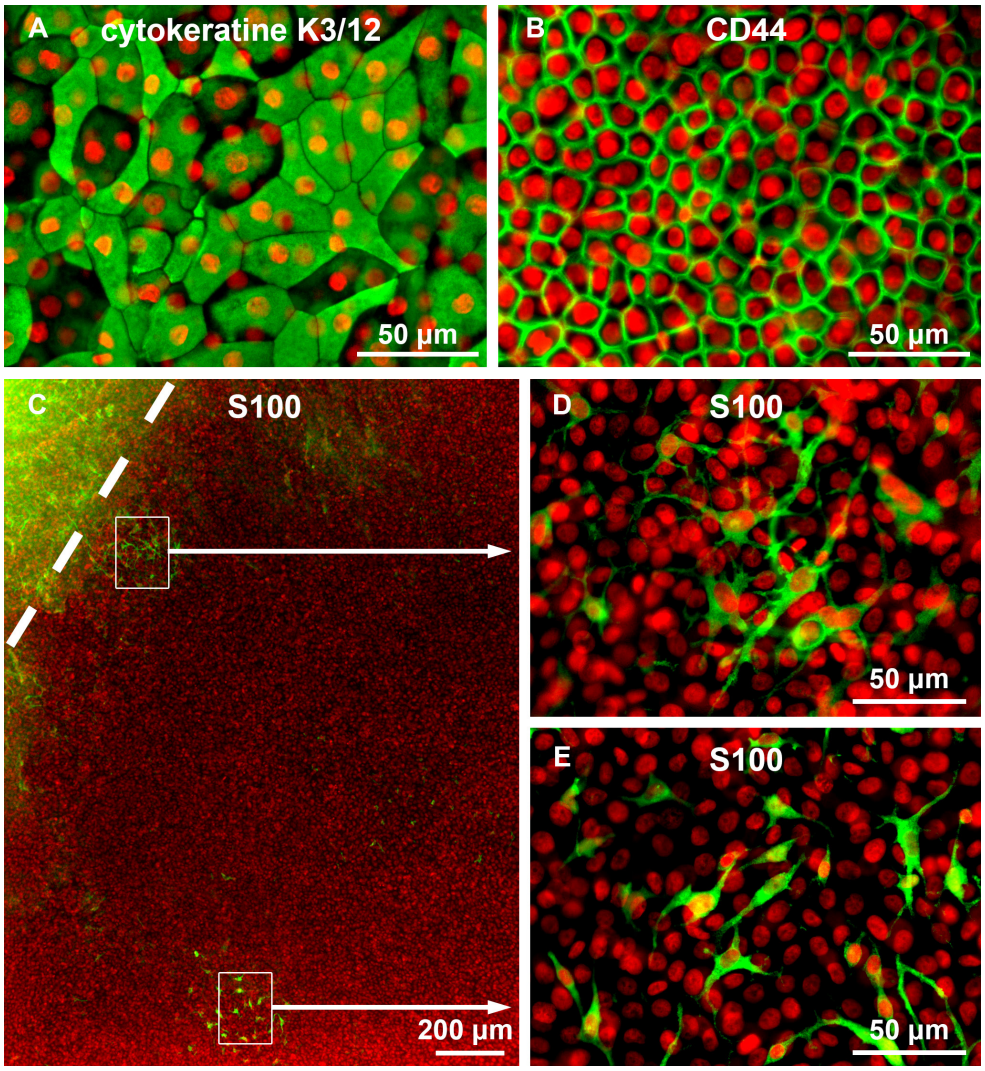

Figure 7. Examples of applications of immunostaining on the flatmounted cornea for the study of the corneal epithelium. **A, B**: High magnification (40X objective) shows the characteristic cell shape of the superficial epithelial cells stained for cytokeratin K3/12 and of the basal epithelial cells stained for CD44. **C**–**E**: Distribution of Langerhans cells, stained for S100B, in the epithelial layer. Low magnification (10X objective) easily reveals different cell locations, most next to the limbus (dash line; **D**) and a few clusters migrating toward the center (**E**). Characteristic cell morphology is perfectly outlined using higher magnification (40X objective). For all five images, the immunostaining is pseudocolored in green, and the nuclei, labeled by Hoechst 33,342, are pseudocolored in red.

provides precise subcellular localization, we demonstrated NCAM expression restricted to the lateral membrane of ECs. This specific membrane labeling reveals the 3D complexity of EC organization, with a progressive increase in the number and tortuosity of intercellular digitations from the apical to the basal cell pole. Interestingly, this technique revealed that discontinuous cell junctions on lateral membranes form inflated pockets between neighboring cells, which had never previously been reported. As numerous ion transporters, such as Na^+/K+ ATPase [29], SLC4A11 [30], and SLC12A2 [31], are localized in the lateral membrane, we hypothesize that this microanatomical organization is involved in endothelial pump mechanisms, particularly the creation of local ionic gradients between compartments.

Although the immunostaining technique on the flat-mounted whole cornea was initially developed for the endothelial monolayer, we noted that this technique also adapted to the multilayered epithelium. Until now, IHC using cross sections was almost the only immunostaining technique used. Here we demonstrated that the en face view can complement the technique, offering for each epithelial layer the same advantages as for the endothelium (observation of large areas and identification of cell subpopulations, and clear subcellular localization). As an example, using S100B labeling of Langerhans cells [32,33], we were able to observe positive cells with a typical phenotype and describe their distribution within the corneal surface, mainly at the limbus as expected but also capable of migrating toward the central epithelium of healthy corneas.

In conclusion, immunostaining on flatmounted cornea differs in several respects from conventional IHC and ICC. An easy, fast method has been developed using fixation with methanol or 0.5% PFA. Room temperature is recommended as the first-line temperature during fixation, instead of the conventional −20 °C for methanol and 4 °C for PFA, and further optimization may be required for certain target proteins. Overview and precise subcellular localization are the main advantages of this technique, for the endothelium and the epithelium, compared to IHC on cross sections of the cornea. The technique might also be useful for studying mono- and multilayered cells of other superficial tissues.

ACKNOWLEDGMENTS

The authors thank Mr. F. Dergandi from the Laboratory of Anatomy of the Pole Santé Innovation for his help with tissue procurement. Dr. Gilles Thuret (gilles.thuret@univ-st-etienne.fr) and Zhiguo He (zhiguo.he@univ-st-etienne.fr) are co-corresponding authors.

REFERENCES

1. Koh SW, Waschek JA. Corneal endothelial cell survival in organ cultures under acute oxidative stress: effect of VIP. Invest Ophthalmol Vis Sci 2000; 41:4085-92. [PMID: 11095600].
2. Koh SW, Chandrasekara K, Abbondandolo CJ, Coll TJ, Rutzen AR. VIP and VIP gene silencing modulation of differentiation marker N-cadherin and cell shape of corneal endothelium in human corneas ex vivo. Invest Ophthalmol Vis Sci 2008; 49:3491-8. [PMID: 18441300].
3. Joyce NC, Harris DL, Zhu CC. Age-related gene response of human corneal endothelium to oxidative stress and DNA damage. Invest Ophthalmol Vis Sci 2011; 52:1641-9. [PMID: 21087955].
4. Azizi B, Ziaei A, Fuchsluger T, Schmedt T, Chen Y, Jurkunas UV. p53-regulated increase in oxidative-stress–induced apoptosis in Fuchs endothelial corneal dystrophy: a native tissue model. Invest Ophthalmol Vis Sci 2011; 52:9291-7. [PMID: 22064994].
5. He Z, Campolmi N, Ha Thi BM, Dumollard JM, Peoc'h M, Garraud O, Piselli S, Gain P, Thuret G. Optimization of immunolocalization of cell cycle proteins in human corneal endothelial cells. Mol Vis 2011; 17:3494-511. [PMID: 22219645].
6. He Z, Campolmi N, Gain P, Minh Hathi B, Dumollard JM, Duband S, Peoc'h M, Piselli S, Garraud O, Thuret G. Revisited Microanatomy of the Corneal Endothelial Periphery: New Evidence for Continuous Centripetal Migration of Endothelial Cells in Humans. Stem Cells 2012; 30:2523-34. [PMID: 22949402].
7. Leong AS. Pitfalls in diagnostic immunohistology. Adv Anat Pathol 2004; 11:86-93. [PMID: 15090844].
8. Burry RW. Controls for immunocytochemistry: an update. J Histochem Cytochem 2011; 59:6-12. [PMID: 20852036].
9. Barry PA, Petroll WM, Andrews PM, Cavanagh HD, Jester JV. The spatial organization of corneal endothelial cytoskeletal proteins and their relationship to the apical junctional complex. Invest Ophthalmol Vis Sci 1995; 36:1115-24. [PMID: 7730021].
10. Kim EK, Geroski DH, Holley GP, Urken SI, Edelhauser HF. Corneal endothelial cytoskeletal changes in F-actin with aging, diabetes, and after cytochalasin exposure. Am J Ophthalmol 1992; 114:329-35. [PMID: 1524124].
11. Borderie VM, Baudrimont M, Vallee A, Ereau TL, Gray F, Laroche L. Corneal endothelial cell apoptosis in patients with Fuchs' dystrophy. Invest Ophthalmol Vis Sci 2000; 41:2501-5. [PMID: 10937560].
12. Foets BJ, van den Oord JJ, Volpes R, Missotten L. In situ immunohistochemical analysis of cell adhesion molecules on human corneal endothelial cells. Br J Ophthalmol 1992; 76:205-9. [PMID: 1382576].
13. Chaloin-Dufau C, Pavitt I, Delorme P, Dhouailly D. Identification of keratins 3 and 12 in corneal epithelium of vertebrates. Epithelial Cell Biol 1993; 2:120-5. [PMID: 7688259].

14. Zhu SN, Nolle B, Duncker G. Expression of adhesion molecule CD44 on human corneas. Br J Ophthalmol 1997; 81:80-4. [PMID: 9135415].

15. Kill IR. Localisation of the Ki-67 antigen within the nucleolus. Evidence for a fibrillarin-deficient region of the dense fibrillar component. J Cell Sci 1996; 109:1253-63. [PMID: 8799815].

16. Zellner M, Winkler W, Hayden H, Diestinger M, Eliasen M, Gesslbauer B, Miller I, Chang M, Kungl A, Roth E, Oehler R. Quantitative validation of different protein precipitation methods in proteome analysis of blood platelets. Electrophoresis 2005; 26:2481-9. [PMID: 15895463].

17. Herskovits TT, Singer SJ, Geiduschek EP. Nonaqueous solutions of DNA. Denaturation in methanol and ethanol. Arch Biochem Biophys 1961; 94:99-114. [PMID: 13713795].

18. Burns JA, Li Y, Cheney CA, Ou Y, Franlin-Pfeifer LL, Kuklin N, Zhang ZQ. Choice of fixative is crucial to successful immunohistochemical detection of phosphoproteins in paraffin-embedded tumor tissues. J Histochem Cytochem 2009; 57:257-64. [PMID: 19001637].

19. Fowler CB, Evers DL, O'Leary TJ, Mason JT. Antigen retrieval causes protein unfolding: evidence for a linear epitope model of recovered immunoreactivity. J Histochem Cytochem 2011; 59:366-81. [PMID: 21411808].

20. Brown D, Lydon J, McLaughlin M, Stuart-Tilley A, Tyszkowski R, Alper S. Antigen retrieval in cryostat tissue sections and cultured cells by treatment with sodium dodecyl sulfate (SDS). Histochem Cell Biol 1996; 105:261-7. [PMID: 9072183].

21. Rajamannan NM, Springett MJ, Pederson LG, Carmichael SW. Localization of caveolin 1 in aortic valve endothelial cells using antigen retrieval. J Histochem Cytochem 2002; 50:617-28. [PMID: 11967273].

22. Allan VJ. Protein localization by fluorescence microscopy. A practical approach. Oxford: Oxford University Press; 1999.

23. Joyce NC. Proliferative capacity of the corneal endothelium. Prog Retin Eye Res 2003; 22:359-89. [PMID: 12852491].

24. Peh GS, Toh KP, Wu FY, Tan DT, Mehta JS. Cultivation of human corneal endothelial cells isolated from paired donor corneas. PLoS ONE 2011; 6:e28310-[PMID: 22194824].

25. Okumura N, Hirano H, Numata R, Nakahara M, Ueno M, Hamuro J, Kinoshita S, Koizumi N. Cell surface markers of functional phenotypic corneal endothelial cells. Invest Ophthalmol Vis Sci 2014; 55:7610-8. [PMID: 25389199].

26. Kreutziger GO. Lateral membrane morphology and gap junction structure in rabbit corneal endothelium. Exp Eye Res 1976; 23:285-93. [PMID: 976372].

27. Hirsch M, Renard G, Faure JP, Pouliquen Y. Study of the ultrastructure of the rabbit corneal endothelium by the freeze-fracture technique: apical and lateral junctions. Exp Eye Res 1977; 25:277-88. [PMID: 590370].

28. Ringvold A, Davanger M, Olsen EG. On the spatial organization of the cornea endothelium. Acta Ophthalmol (Copenh) 1984; 62:911-8. [PMID: 6524316].

29. McCartney MD, Wood TO, McLaughlin BJ. Immunohistochemical localization of ATPase in human dysfunctional corneal endothelium. Curr Eye Res 1987; 6:1479-86. [PMID: 2827961].

30. Jalimarada SS, Ogando DG, Vithana EN, Bonanno JA. Ion transport function of SLC4A11 in corneal endothelium. Invest Ophthalmol Vis Sci 2013; 54:4330-40. [PMID: 23745003].

31. Jelamskii S, Sun XC, Herse P, Bonanno JA. Basolateral Na(+)-K(+)-2Cl(-) cotransport in cultured and fresh bovine corneal endothelium. Invest Ophthalmol Vis Sci 2000; 41:488-95. [PMID: 10670480].

32. Takahashi K, Isobe T, Ohtsuki Y, Sonobe H, Takeda I, Akagi T. Immunohistochemical localization and distribution of S-100 proteins in the human lymphoreticular system. Am J Pathol 1984; 116:497-503. [PMID: 6476082].

33. Nishikawa Y, Sato H, Oka T, Yoshino T, Takahashi K. Immunohistochemical discrimination of plasmacytoid dendritic cells from myeloid dendritic cells in human pathological tissues. Journal of clinical and experimental hematopathology JCEH 2009; 49:23-31. [PMID: 19474514].

Articles are provided courtesy of Emory University and the Zhongshan Ophthalmic Center, Sun Yat-sen University, P.R. China. The print version of this article was created on 30 December 2015. This reflects all typographical corrections and errata to the article through that date. Details of any changes may be found in the online version of the article.